Inverse Engineering

George S. Dulikravich[1], Helcio R. B. Orlande[2] and Brian H. Dennis[3]

[1]Florida International University, Department of Mechanical & Materials Eng.
10555 West Flagler Street, Room EC 3474, Miami, Florida 33174, U.S.A.
[2]Federal University of Rio de Janeiro, Department of Mechanical Eng., COPPE,
Cid. Universitaria, Cx. Postal 68503, Rio de Janeiro, RJ, 21941-972, Brazil
[3]Department of Mechanical and Aerospace Eng., University of Texas at Arlington,
Arlington, Texas 78712, U.S.A.
dulikrav@fiu.edu, helcio@serv.com.ufrj.br,
dennis@mae.uta.edu

Inverse problems are rapidly becoming a multi-disciplinary field with many practical engineering applications. The objective of this lecture is to present several such multi-disciplinary concepts and applications. In some examples, sophisticated regularization formulations were used. In other examples, different optimization algorithms were used as tools to solve *de facto* inverse problems. Due to the mathematical complexity of these multi-disciplinary and often multi-scale inverse problems, the most widely acceptable formulations eventually result in a need for minimization of a certain norm or a simultaneous extremization of several such norms. These single-objective and multi-objective minimization problems are then solved using appropriate robust evolutionary optimization algorithms. Specifically, we focus here on inverse problems of determining spatial distribution of a heat source for specified thermal boundary conditions, finding simultaneously thermal and stress/deformation boundary conditions on inaccessible boundaries, and determining chemical compositions of steel alloys for specified multiple properties.

1 Introduction

If the inverse problem involves the estimation of only few unknown parameters, such as the estimation of a thermal conductivity value from the transient temperature measurements in a solid, the averaging capabilities provided by the minimization of objective functions such as *ordinary least squares norm* can result in stable solutions. Indeed, other similar objective functions can be defined that are based on statistical fundamentals regarding the measurement errors and the unknown parameters, which are also capable of providing stable solutions for the parameter estimation problem [1,2]. However, if the inverse problem involves the estimation of a large number of parameters, such as the recovery of the unknown transient heat flux components $f(t_i) \equiv f_i$ at times t_i, $i = 1,\ldots,I$, excursions and oscillations of the solution may occur. Therefore, the solution of this type of inverse problems,

known as function estimation problems, requires special *regularization* (stabilization) *techniques*. Here, we used *Alifanov's Iterative Regularization Method* based on the conjugate gradient method of minimization, as well as on the use of an adjoint problem for the computation of the gradient direction [3-17]. Alternatively, one could use boundary regularization methods [18-21] with finite elements.

2 Conjugate Gradient Method of Function Estimation with Adjoint Problem Formulation

First, let us consider an inverse problem dealing with the estimation of a distributed heat source term in a two-region heat conduction problem. The physical problem of interest is typical of the manufacturing of Micro-Electro-Mechanical Systems (MEMS) and is called Hot Embossing *Microfabrication Microreplication* (HEMM). Such technique consists of pressing a mold on a substrate under a prescribed thermal history and can also be used for the fabrication of macro-scale parts. In general, the polymer substrate and the mold are heated to a temperature just above the polymer glass transition temperature. The mold is then pressed on the polymer until features get replicated and then both the mold and the substrate are cooled down to a temperature below the glass transition temperature for deembossing [17]. The estimation of the source term within the mold will be accomplished by using the temperature variation at selected points within the substrate. Such an inverse problem can be aimed at the *identification* of the unknown source term by using temperature measurements within the substrate, or, alternatively, at the *design* of the source term that will result in a prescribed temperature history required for the HEMM technique.

The physical problem considered in this work consists of the two-dimensional heat conduction in two contacting rectangular regions, as depicted in Figure 1. The widths of both regions are a, while the thickness of region A is b and the thickness of region B is (c-b). Regions A and B are initially at the uniform temperatures T_{0A} and T_{0B}, respectively. For $t > 0$, the two regions are placed in contact and heat is generated in region B at a volumetric rate $g(x,y,t)$. The contact conductance at the interface between the two regions, h_c, is supposed to be uniform and the other boundaries of regions A and B are supposed to be insulated.

The mathematical model utilizes the following dimensionless groups

$$\theta_A(X,Y,\tau)=\frac{T_A(x,y,t)-T_{0A}}{T_{0A}}, \qquad \theta_B(X,Y,\tau)=\frac{T_B(x,y,t)-T_{0A}}{T_{0A}}, \tag{1.a-b}$$

$$\tau=\frac{\alpha_A\, t}{a^2}, \quad X=\frac{x}{a}, \quad Y=\frac{y}{a} \tag{1.c-e}$$

$$G(X,Y,\tau)=\frac{g(x,y,t)a^2}{k_A T_{0A}}, \; Bi=\frac{h_c\, a}{k_A}, \; K=\frac{k_B}{k_A}, \; \Lambda=\frac{\alpha_B}{\alpha_A}, \; B=\frac{b}{a}, \; C=\frac{c}{a} \tag{1.f-k}$$

where k is the thermal conductivity and α is the thermal diffusivity.

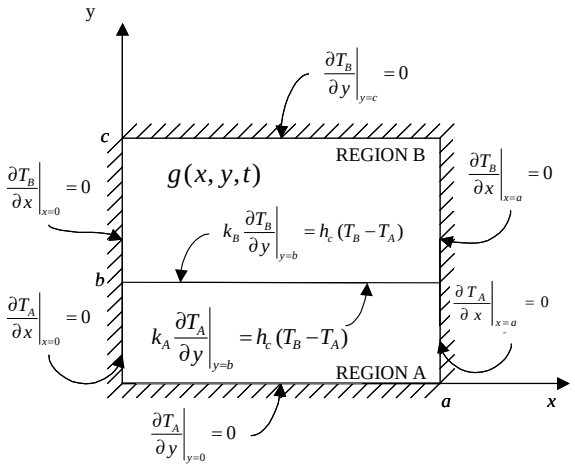

Fig. 1. Geometry, coordinates and boundary conditions.

By assuming that the thermal properties of regions A and B are constant, the mathematical formulation for this problem is given in dimensionless form as:

Region A:

$$\frac{\partial \theta_A}{\partial \tau} = \frac{\partial^2 \theta_A}{\partial X^2} + \frac{\partial^2 \theta_A}{\partial Y^2} \qquad \text{in } 0 < X < 1,\ 0 < Y < B,\ \text{for } \tau > 0 \qquad (2.a)$$

$$\left.\frac{\partial \theta_A}{\partial X}\right|_{X=0} = 0 \qquad \text{at } X = 0,\ 0 < Y < B,\ \text{for } \tau > 0 \qquad (2.b)$$

$$\left.\frac{\partial \theta_A}{\partial X}\right|_{X=1} = 0 \qquad \text{at } X = 1,\ 0 < Y < B,\ \text{for } \tau > 0 \qquad (2.c)$$

$$\left.\frac{\partial \theta_A}{\partial Y}\right|_{Y=0} = 0 \qquad \text{at } Y = 0,\ 0 < X < 1,\ \text{for } \tau > 0 \qquad (2.d)$$

$$\left.\frac{\partial \theta_A}{\partial Y}\right|_{Y=B} = Bi(\theta_B - \theta_A) \qquad \text{at } Y = B,\ 0 < X < 1,\ \text{for } \tau > 0 \qquad (2.e)$$

$$\theta_A(X,Y,0) = 0 \qquad \text{for } \tau = 0,\ \text{in } 0 < X < 1,\ 0 < Y < B \qquad (2.f)$$

Region B

$$\frac{1}{\Lambda}\frac{\partial \theta_B}{\partial \tau} = \frac{\partial^2 \theta_B}{\partial X^2} + \frac{\partial^2 \theta_B}{\partial Y^2} + \frac{G(X,Y,\tau)}{K} \qquad 0 < X < 1,\ B < Y < C,\ \text{for } \tau > 0 \qquad (3.a)$$

$$\left.\frac{\partial \theta_B}{\partial X}\right|_{X=0} = 0 \qquad \text{at } X = 0,\ B < Y < C,\ \text{for } \tau > 0 \qquad (3.b)$$

$$\left.\frac{\partial \theta_B}{\partial X}\right|_{X=1} = 0 \qquad \text{at } X = 1,\ B < Y < C,\ \text{for } \tau > 0 \qquad (3.c)$$

$$\left.\frac{\partial \theta_B}{\partial Y}\right|_{Y=B} = \frac{1}{K} Bi(\theta_B - \theta_A) \qquad \text{at } Y = B,\ 0 < X < 1, \text{ for } \tau > 0 \qquad (3.d)$$

$$\left.\frac{\partial \theta_B}{\partial Y}\right|_{Y=C} = 0 \qquad \text{at } Y = C,\ 0 < X < 1, \text{ for } \tau > 0 \qquad (3.e)$$

$$\theta_B(X,Y,0) = \theta_{0B} \qquad \text{for } \tau = 0, \text{ in } 0 < X < 1\ ,\ B < Y < C \qquad (3.f)$$

The problem defined by eqns. (2.a-f) and (3.a-f), with known initial and boundary conditions, contact conductance, thermophysical properties and source term constitutes a *direct problem* that is concerned with the determination of the transient temperature fields $\theta_A(X,Y,\tau)$ and $\theta_B(X,Y,\tau)$.

For the *inverse problem* of interest here, the heat source term $G(X,Y,\tau)$ is regarded as unknown, while the other quantities appearing in the formulation of the direct problem are considered to be known. For the solution of the inverse problem, we consider the available transient temperature histories $\mu_{Am}(\tau)$ at positions locations (X_m,Y_m), $m = 1,..,M$, in region A, as well as $\mu_{Bn}(\tau)$, $n = 1,..,N$, at locations (X_n,Y_n) in region B. For the *design inverse problem*, $\mu_{Am}(\tau)$ and $\mu_{Bn}(\tau)$ represent desired temperatures for the fabrication procedure, while for the *identification inverse problem*, $\mu_{Am}(\tau)$ and $\mu_{Bn}(\tau)$ represent temperature measurements. The measurements contain errors, which are supposed to be additive, uncorrelated, normally distributed, with known and constant standard deviation and zero mean.

For the estimation of the unknown function $G(X,Y,\tau)$, we make no *a priori* assumption regarding its functional form, except that it belongs to the Hilbert space of square-integrable functions [2-16] in the domain $0 < X < 1$, $B < Y < C$ and $0 < \tau < \tau_f$, where τ_f is the duration of the time interval of concern for the inverse analysis. For the solution of the present inverse problem, we consider the minimization of the following functional.

$$S[G(X,Y,\tau)] = \sum_{m=1}^{M} \int_{\tau=0}^{\tau_f} [\mu_{Am}(\tau) - \theta_A(X_m,Y_m,\tau;G)]^2\, d\tau + \sum_{n=1}^{N} \int_{\tau=0}^{\tau_f} [\mu_{Bn}(\tau) - \theta_B(X_n,Y_n,\tau;G)]^2\, d\tau \qquad (4)$$

For the minimization of the objective functional (4) two auxiliary problems are developed, namely the sensitivity problem and the adjoint problem. The sensitivity problem is used to determine the variations $\Delta\theta_A(X,Y,\tau)$ and $\Delta\theta_B(X,Y,\tau)$ when the unknown function is perturbed by $\Delta G(X,Y,\tau)$ [2-16]. The sensitivity problem is derived by substituting into the direct problem given by eqns. (2.a-f) and (3.a-f), $\theta_A(X,Y,\tau)$ by $[\theta_A(X,Y,\tau) + \Delta\theta_A(X,Y,\tau)]$, $\theta_B(X,Y,\tau)$ by $[\theta_B(X,Y,\tau) + \Delta\theta_B(X,Y,\tau)]$ and $G(X,Y,\tau)$ by $[G(X,Y,\tau) + \Delta G(X,Y,\tau)]$. The original direct problem is then subtracted from the resulting equations in order to obtain the following sensitivity problem:

Region A:

$$\frac{\partial \Delta\theta_A}{\partial \tau} = \frac{\partial^2 \Delta\theta_A}{\partial X^2} + \frac{\partial^2 \Delta\theta_A}{\partial Y^2} \qquad \text{in } 0 < X < 1\ ,\ 0 < Y < B, \text{ for } \tau > 0 \qquad (5.a)$$

$$\left.\frac{\partial \Delta\theta_A}{\partial X}\right|_{X=0} = 0 \qquad \text{at } X = 0\,,\ 0 < Y < B\,, \text{ for } \tau > 0 \qquad (5.b)$$

$$\left.\frac{\partial \Delta\theta_A}{\partial X}\right|_{X=1} = 0 \qquad \text{at } X = 1\,,\ 0 < Y < B\,, \text{ for } \tau > 0 \qquad (5.c)$$

$$\left.\frac{\partial \Delta\theta_A}{\partial Y}\right|_{Y=0} = 0 \qquad \text{at } Y = 0,\ 0 < X < 1, \text{ for } \tau > 0 \qquad (5.d)$$

$$\left.\frac{\partial \Delta\theta_A}{\partial Y}\right|_{Y=B} = Bi(\Delta\theta_B - \Delta\theta_A) \quad \text{at } Y = B,\ 0 < X < 1, \text{ for } \tau > 0 \qquad (5.e)$$

$$\Delta\theta_A(X,Y,0) = 0 \qquad \text{for } \tau = 0, \text{ in } 0 < X < 1\,,\ 0 < Y < B \qquad (5.f)$$

Region B:

$$\frac{1}{\Lambda}\frac{\partial \Delta\theta_B}{\partial \tau} = \frac{\partial^2 \Delta\theta_B}{\partial X^2} + \frac{\partial^2 \Delta\theta_B}{\partial Y^2} + \frac{\Delta G(X,Y,\tau)}{K} \quad 0 < X < 1\,,\ B < Y < C\,, \text{ for } \tau > 0 \qquad (6.a)$$

$$\left.\frac{\partial \Delta\theta_B}{\partial X}\right|_{X=0} = 0 \qquad \text{at } X = 0\,,\ B < Y < C, \text{ for } \tau > 0 \qquad (6.b)$$

$$\left.\frac{\partial \Delta\theta_B}{\partial X}\right|_{X=1} = 0 \qquad \text{at } X = 1\,,\ B < Y < C, \text{ for } \tau > 0 \qquad (6.c)$$

$$\left.\frac{\partial \Delta\theta_B}{\partial Y}\right|_{Y=B} = \frac{1}{K} Bi(\Delta\theta_B - \Delta\theta_A) \qquad \text{at } Y = B,\ 0 < X < 1, \text{ for } \tau > 0 \qquad (6.d)$$

$$\left.\frac{\partial \Delta\theta_B}{\partial Y}\right|_{Y=C} = 0 \qquad \text{at } Y = C,\ 0 < X < 1, \text{ for } \tau > 0 \qquad (6.e)$$

$$\Delta\theta_B(X,Y,0) = 0 \qquad \text{for } \tau = 0, \text{ in } 0 < X < 1\,,\ B < Y < C \qquad (6.f)$$

The adjoint problem is derived by multiplying the governing equations of the direct problem, eqns. (2.a) and (3.a) by the Lagrange multipliers $\lambda_A(X,Y,\tau)$ and $\lambda_B(X,Y,\tau)$, respectively. The equations are then integrated in the spatial and time domains that are valid and added to the original functional (4). The directional derivative of the extended functional in the direction of the perturbation of the unknown function is then obtained and the resultant expression, after some lengthy

but straightforward manipulations, is allowed to go to zero [2-16]. The following adjoint problem for the determination of the Lagrange multipliers $\lambda_A(X,Y,\tau)$ and $\lambda_B(X,Y,\tau)$ results in

Region A:

$$-\frac{\partial \lambda_A}{\partial \tau}=\frac{\partial^2 \lambda_A}{\partial X^2}+\frac{\partial^2 \lambda_A}{\partial Y^2}+2\sum_{m=1}^{M}[\theta_A(X,Y,\tau)-\mu_{Am}(\tau)]\,\delta(X-X_m)\,\delta(Y-Y_m)$$

$$\text{in } 0<X<1\,,\ 0<Y<B\,,\ 0<\tau<\tau_f \tag{7.a}$$

$$\left.\frac{\partial \lambda_A}{\partial X}\right|_{X=0}=0 \qquad \text{at } X=0\,,\ 0<Y<B\,,\ 0<\tau<\tau_f \tag{7.b}$$

$$\left.\frac{\partial \lambda_A}{\partial X}\right|_{X=1}=0 \qquad \text{at } X=1\,,\ 0<Y<B\,,\ 0<\tau<\tau_f \tag{7.c}$$

$$\left.\frac{\partial \lambda_A}{\partial Y}\right|_{Y=0}=0 \qquad \text{at } Y=0,\ 0<X<1,\ 0<\tau<\tau_f \tag{7.d}$$

$$\left.\frac{\partial \lambda_A}{\partial Y}\right|_{Y=B}=Bi\left(\frac{\lambda_B}{K}-\lambda_A\right) \quad \text{at } Y=B,\ 0<X<1,\ 0<\tau<\tau_f \tag{7.e}$$

$$\lambda_A(X,Y,\tau_f)=0 \qquad \text{for } \tau=\tau_f,\ \text{in } 0<X<1\,,\ 0<Y<B \tag{7.f}$$

Region B:

$$-\frac{\partial \lambda_B}{\partial \tau}=\frac{\partial^2 \lambda_B}{\partial X^2}+\frac{\partial^2 \lambda_B}{\partial Y^2}+2\sum_{n=1}^{N}[\theta_B(X,Y,\tau)-\mu_{Bn}(\tau)]\,\delta(X-X_n)\,\delta(Y-Y_n)$$

$$\text{in } 0<X<1\,,\ B<Y<C\,,\ 0<\tau<\tau_f \tag{8.a}$$

$$\left.\frac{\partial \lambda_B}{\partial X}\right|_{X=0}=0 \qquad \text{at } X=0\,,\ B<Y<C,\ 0<\tau<\tau_f \tag{8.b}$$

$$\left.\frac{\partial \lambda_B}{\partial X}\right|_{X=1}=0 \qquad \text{at } X=1\,,\ B<Y<C,\ 0<\tau<\tau_f \tag{8.c}$$

$$\left.\frac{\partial \lambda_B}{\partial Y}\right|_{Y=B}=Bi\left(\frac{\lambda_B}{K}-\lambda_A\right) \quad \text{at } Y=B,\ 0<X<1,\ 0<\tau<\tau_f \tag{8.d}$$

$$\left.\frac{\partial \lambda_B}{\partial Y}\right|_{Y=C} = 0 \qquad \text{at } Y = C,\ 0 < X < 1,\ 0 < \tau < \tau_f \tag{8.e}$$

$$\lambda_B(X, Y, \tau_f) = 0 \qquad \text{for } \tau = \tau_f, \text{ in } 0 < X < 1,\ B < Y < C \tag{8.f}$$

By applying the limiting process used to obtain the adjoint problem, the directional derivative of the objective functional along the direction of the perturbation $\Delta G(X,Y,\tau)$ reduces to

$$\Delta S[G(X,Y,\tau)] = \int_{\tau=0}^{\tau_f} \int_{Y=B}^{C} \int_{X=0}^{1} \frac{\lambda_B(X,Y,\tau)}{K} \Delta G(X,Y,\tau)\, dX\, dY\, d\tau \tag{9.a}$$

We now invoke the hypothesis that the unknown function belongs to the Hilbert space of square integrable functions in the domain $0 < X < 1$, $B < Y < C$ and $0 < \tau < \tau_f$, so that we can write such directional derivative as

$$\Delta S[G(X,Y,\tau)] = \int_{\tau=0}^{\tau_f} \int_{Y=B}^{C} \int_{X=0}^{1} \nabla S[G(X,Y,\tau)] \Delta G(X,Y,\tau)\, dX\, dY\, d\tau \tag{9.b}$$

By comparing eqns. (9.a) and (9.b) we obtain the gradient direction as

$$\nabla S[G(X,Y,\tau)] = \frac{\lambda_B(X,Y,\tau)}{K} \tag{10}$$

The iterative procedure of the conjugate gradient method, as applied to the estimation of the function $G(X,Y,\tau)$, is given by

$$G^{k+1}(X,Y,\tau) = G^k(X,Y,\tau) - \beta^k\ d^k(X,Y,\tau) \tag{11.a}$$

where the superscript k denotes the number of iterations and β^k is the search step size. The direction of descent, d^k, is obtained as a linear combination of the gradient direction at iteration k with directions of descent at previous iterations. It is given as [2-16]

$$d^k(X,Y,\tau) = \nabla S[G^k(X,Y,\tau)] + \gamma^k d^{k-1}(X,Y,\tau) \tag{11.b}$$

Different expressions are available in the literature for the conjugation coefficient, γ^k. In this work, we use the so-called Fletcher-Reeves version of the conjugate gradient method, where the conjugation coefficient is given as [2-16]

$$\gamma^k = \frac{\int_{\tau=0}^{\tau_f} \int_{Y=B}^{C} \int_{X=0}^{1} \{\nabla S[G^k(X,Y,\tau)]\}^2\, dX\, dY\, d\tau}{\int_{\tau=0}^{\tau_f} \int_{Y=B}^{C} \int_{X=0}^{1} \{\nabla S[G^{k-1}(X,Y,\tau)]\}^2\, dX\, dY\, d\tau} \qquad k = 1,2,3,\ldots \text{with } \gamma^0 = 0 \tag{11.c}$$

The search step size is obtained by minimizing the objective functional with respect to β^k at each iteration [2-16]. The following expression results for the present inverse problem

$$\beta^k = \frac{\sum_{m=1}^{M}\int_{\tau=0}^{\tau_f}[\theta_A(X_m,Y_m,\tau;G)-\mu_{Am}(\tau)]\Delta\theta_A(X_m,Y_m,\tau;d^k)d\tau+\sum_{n=1}^{N}\int_{\tau=0}^{\tau_f}[\theta_B(X_n,Y_n,\tau;G)-\mu_{Bn}(\tau)]\Delta\theta_B(X_n,Y_n,\tau;d^k)d\tau}{\sum_{m=1}^{M}\int_{\tau=0}^{\tau_f}[\Delta\theta_A(X_m,Y_m,\tau;d^k)]^2\,d\tau+\sum_{n=1}^{N}\int_{\tau=0}^{\tau_f}[\Delta\theta_B(X_n,Y_n,\tau;d^k)]^2 d\tau} \tag{11.d}$$

where $\Delta\theta_A(X,Y,\tau;d^k)$ and $\Delta\theta_B(X,Y,\tau;d^k)$ are the solutions of the sensitivity problem given by eqns. (5.a-f) and (6.a-f), obtained by setting $\Delta G(X,Y,\tau) = d^k(X,Y,\tau)$.

After developing the expressions for the search step size and for the gradient direction, the iterative procedure of the conjugate gradient method given by eqns. (11.a-d) can be applied until a suitable convergence criterion is satisfied. The minimization of the objective functional with the conjugate gradient method and adjoint problem formulation can be suitably arranged in a computational algorithm, which is omitted here for the sake of brevity. The reader should consult references [2-16] for further details. In this paper, the iterative procedure was stopped when the objective functional given by equation (4) became sufficiently small. The *discrepancy principle* [2-16] was used to specify the tolerance for the stopping criterion if temperature measurements containing random errors were used for the inverse identification of the source term. For the inverse design problem, the tolerance was specified as a small number.

We consider here the inverse problem of designing the heat source term in the mold so that the temperature at the mold/substrate interface follows a desired history imposed by the manufacturing process. We assumed the substrate and the mold to have the following properties [17]: $k_A = 0.19\ W\,m^{-1}\,K^{-1}$, $\alpha_A = 1.144 \times 10^{-7}\ m^2\,s^{-1}$, $k_B = 14.8\ W\,m^{-1}\,K^{-1}$ and $\alpha_B = 9.056 \times 10^{-6}\ m^2\,s^{-1}$, that is, $K = 77.89$ and $\Lambda = 79.16$. Both regions A and B were initially at the same temperature $T_{0A} = T_{0B} = 27\ ^oC$. The mold and substrate dimensions (Figure 1) were $a = 0.075\ m$, $b = 0.001\ m$,$(b\text{-}c) = 0.065\ m$ and the duration of the hot embossing process was taken as 1400 s, that is, $B = 0.013$, $C = 1$ and $\tau_f = 0.028$. Uniform interface temperature and perfect contact between regions A and B were assumed for the results presented here. Figure 2 presents the desired temperature variation at the interface between regions A and B, as well as the calculated temperatures obtained with the heat source term that resulted from the solution of the present inverse design problem. The agreement between desired and calculated temperatures is perfect within the graph scale, despite the fact that the desired temperature variation contains sharp variations. Figures 3.a-d present the resultant heat source term at positions $Y = 0.013$, 0.34, 0.67 and 1.0, respectively. Each of these figures shows the results for $X = 0.02$, 0.22, 0.42 and 0.98. We note in figures 3.a-d that the source term found from the design procedure does not vary along the X direction for such test case. In addition, periods of heating (positive source) and cooling (negative source) can be clearly identified, as required for the sharp increase and decrease in temperature at times $\tau = 0$ and $\tau = 0.02$, respectively (see Figure 2). The obtained results reveal that the conjugate gradient method of function estimation is capable of providing smooth and stable solutions for the source term. We note that the present inverse design analysis assumes that the source term is continuous within the mold, but, for practical implementation discrete heat sources and cooling channels

will be required. The results obtained with the conjugate gradient method of function estimation permit the selection of the number and position of the heat sources and cooling channels, as well as the heating power, cooling fluid temperature and convective heat transfer coefficient, which will result in the desired interface temperature variation.

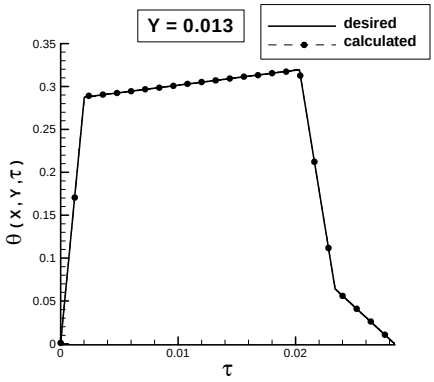

Fig. 2. Comparison between desired and calculated interface temperatures.

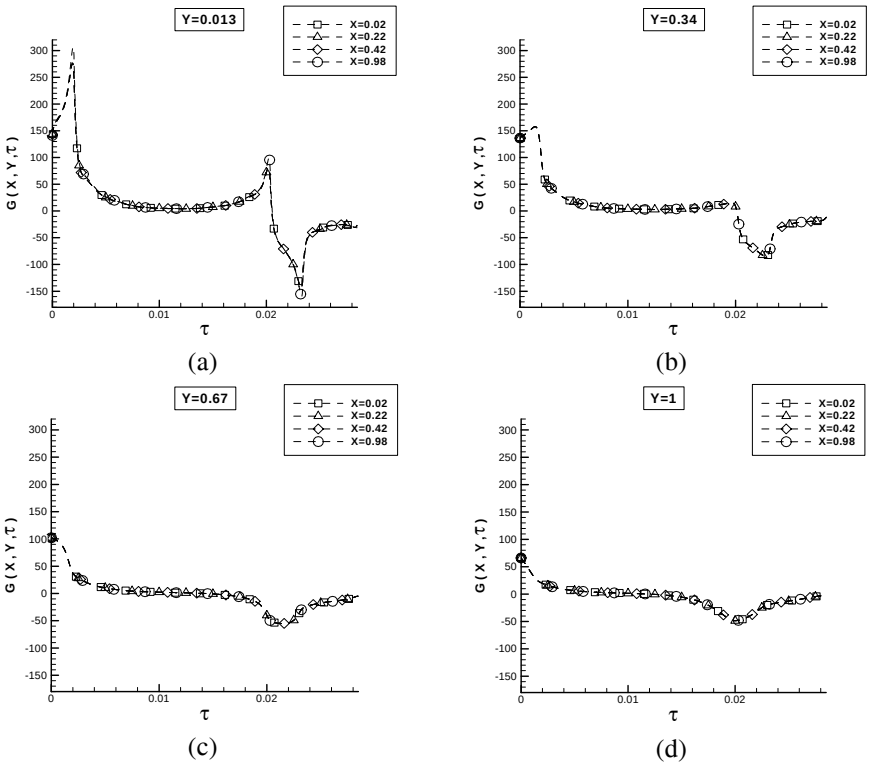

Fig. 3. Inverse solution at: (a) $Y = 0.013$, (b) $Y = 0.34$, (c) $Y = 0.67$, (d) $Y = 1$.

3 A Finite Element Formulation for Finding Unknown Boundary Conditions in 3-D Steady Thermoelasticity

It is often difficult or even impossible to place temperature probes, heat flux probes, or strain gauges on certain parts of a surface of a solid body. This can be due to its small size, geometric inaccessibility, or exposure to a hostile environment. For inverse problems, the unknown boundary conditions on parts of the boundary can be determined by providing overspecified boundary conditions (enforcing both Dirichlet and Neumann type boundary conditions) on at least some of the remaining portions of the boundary, and providing either Dirichlet or Neumann type boundary conditions on the rest of the boundary [22-24]. It is possible, after a series of algebraic manipulations, to transform the original system of equations into a system which enforces the overspecified boundary conditions and includes the unknown boundary conditions as a part of the unknown solution vector. This formulation is an adaptation of a method used by Martin and Dulikravich [25,26] for the inverse detection of boundary conditions in steady heat conduction. Specifically, this work represents an extension of the work presented by the authors [18,19,21].

In the case of steady combined thermal and elastic problems, the objective of the inverse problem is to determine displacements, surface stresses, heat fluxes, and temperatures on boundaries where they are unknown. The problem of inverse determination of unknown boundary conditions in two-dimensional steady heat conduction has been solved by a variety of methods [18, 20-25]. Similarly, a separate inverse boundary condition determination problem in linear elastostatics has been solved by different methods [26]. The inverse boundary condition determination problem for combined steady thermoelasticity was also solved for several two-dimensional and three-dimensional problems [18, 21]. A 3-D finite element formulation is presented here that allows one to solve this inverse problem in a direct manner by over-specifying boundary conditions on boundaries where that information is available. Our objective is to develop and demonstrate an approach for the prediction of thermal and elastic boundary conditions on parts of a three-dimensional solid body surface by using a finite element approach (FEA).

It should be pointed out that the method for the solution of inverse problems to be discussed here is different from the approach based on boundary element method that has been used separately in linear heat conduction [24] and linear elasticity [26].

3.1 FEM formulation for thermoelasticity

The Navier equations for linear static deformations u, v, w in three-dimensional Cartesian x, y, z coordinates are

$$(\lambda + G)\left(\frac{\partial^2 u}{\partial x^2} + \frac{\partial^2 v}{\partial x \partial y} + \frac{\partial^2 w}{\partial x \partial z}\right) + G\nabla^2 u + X = 0 \qquad (12)$$

$$(\lambda+G)\left(\frac{\partial^2 u}{\partial x\partial y}+\frac{\partial^2 v}{\partial y^2}+\frac{\partial^2 w}{\partial y\partial z}\right)+G\nabla^2 v+Y=0 \tag{13}$$

$$(\lambda+G)\left(\frac{\partial^2 u}{\partial x\partial z}+\frac{\partial^2 v}{\partial y\partial z}+\frac{\partial^2 w}{\partial z^2}\right)+G\nabla^2 w+Z=0 \tag{14}$$

where,

$$\lambda=\frac{E\nu}{(1+\nu)(1-2\nu)}, \qquad G=\frac{E}{2(1+\nu)} \tag{15}$$

Here, X, Y, Z are body forces per unit volume due to stresses from thermal expansion, ν is the Poisson's ratio, G is the shear modulus, E is the modulus of elasticity, and λ is Lame's constant.

$$X=-(3\lambda+2G)\frac{\partial\alpha\Delta\theta}{\partial x} \tag{16}$$

$$Y=-(3\lambda+2G)\frac{\partial\alpha\Delta\theta}{\partial y} \tag{17}$$

$$Z=-(3\lambda+2G)\frac{\partial\alpha\Delta\theta}{\partial z} \tag{18}$$

Here, α is the coefficient of three-dimensional thermal expansion and θ is the temperature. This system of differential equations is discretized using the typical Galerkin finite element approach [28, 29]. The approach leads to a local stiffness matrix, $\left[K^e\right]$, and a force per unit volume vector, $\left\{f^e\right\}$, which are determined for each element in the domain and then assembled into the global system

$$[K]\{\delta\}=\{F\} \tag{19}$$

After applying boundary conditions, the global displacements are found by solving this system of linear algebraic equations. The stresses, $\{\sigma\}$, can then be found in by differentiating the displacements, $\{\delta\}$.

3.2 FEM formulation for the thermal problem

The temperature distribution throughout the domain can be found by solving Poisson's equation for steady linear heat conduction with a distributed steady heat source function, Q, and thermal conductivity coefficient, k.

$$-k\left(\frac{\partial^2\theta}{\partial x^2}+\frac{\partial^2\theta}{\partial y^2}+\frac{\partial^2\theta}{\partial z^2}\right)=Q \tag{20}$$

Applying the Galerkin finite element method over an element results in the local stiffness matrix, $\left[K_c^e\right]$, and heat flux vector, $\left\{Q^e\right\}$, which determined for each element in the domain and then assembled into the global system

$$[K_c]\{\theta\} = \{Q\} \tag{21}$$

3.3 Direct and inverse formulations

The above equations for steady thermoelasticity were discretized by using a Galerkin's finite element method. This results in two linear systems of algebraic equations

$$[K]\{\delta\} = \{F\}, \qquad [K_c]\{\theta\} = \{Q\} \tag{22}$$

The system is typically large, sparse, symmetric, and positive definite. Once the global system has been formed, the boundary conditions are applied. For a well-posed analysis (direct) problem, the boundary conditions must be known on all boundaries of the domain. For heat conduction, either the temperature, θ_s, or the heat flux, Q_s, must be specified at each point of the boundary.

For an inverse problem, the unknown boundary conditions on parts of the boundary can be determined by over-specifying the boundary conditions (enforcing both Dirichlet and Neumann type boundary conditions) on at least some of the remaining portions of the boundary, and providing either Dirichlet or Neumann type boundary conditions on the rest of the boundary. It is possible, after a series of algebraic manipulations, to transform the original system of equations into a system which enforces the over-specified boundary conditions and includes the unknown boundary conditions as a part of the unknown solution vector.

For example, consider the linear system for heat conduction on a tetrahedral finite element with boundary conditions given at nodes 1 and 4.

$$\begin{bmatrix} K_{11} & K_{12} & K_{13} & K_{14} \\ K_{21} & K_{22} & K_{23} & K_{24} \\ K_{31} & K_{32} & K_{33} & K_{34} \\ K_{41} & K_{42} & K_{43} & K_{44} \end{bmatrix} \begin{Bmatrix} \theta_1 \\ \theta_2 \\ \theta_3 \\ \theta_4 \end{Bmatrix} = \begin{Bmatrix} Q_1 \\ Q_2 \\ Q_3 \\ Q_4 \end{Bmatrix} \tag{23}$$

As an example of an inverse problem, one could specify both the temperature, θ_s, and the heat flux, Q_s, at node 1, flux only at nodes 2 and 3, and assume the boundary conditions at node 4 as being unknown. The original system of equations (23) can be modified by adding a row and a column corresponding to the additional equation for the over-specified flux at node 1 and the additional unknown due to the unknown boundary flux at node 4. The result is

$$\begin{bmatrix} 1 & 0 & 0 & 0 & 0 \\ K_{21} & K_{22} & K_{23} & K_{24} & 0 \\ K_{31} & K_{32} & K_{33} & K_{34} & 0 \\ K_{41} & K_{42} & K_{43} & K_{44} & -1 \\ K_{11} & K_{12} & K_{13} & K_{14} & 0 \end{bmatrix} \begin{Bmatrix} \theta_1 \\ \theta_2 \\ \theta_3 \\ \theta_4 \\ Q_4 \end{Bmatrix} = \begin{Bmatrix} Q_s \\ Q_2 \\ Q_3 \\ 0 \\ Q_s \end{Bmatrix} \tag{24}$$

The resulting systems of equations will remain sparse, but will be non-symmetric and possibly rectangular (instead of square) depending on the ratio of the number of known to unknown boundary conditions.

3.4 Regularization strategies

A regularization method was applied to the solution of the systems of equations in attempts to increase the method's tolerance for measurement errors in the over-specified boundary conditions. Different regularization methods for the 3-D formulation were given previously [21]. Here we consider the regularization of the inverse heat conduction problem.

The general form of a regularized system is given as [30]

$$\begin{bmatrix} K_c \\ \Lambda D \end{bmatrix} \{\theta\} = \begin{Bmatrix} Q \\ 0 \end{Bmatrix} \tag{25}$$

The traditional Tikhonov regularization is obtained when the damping matrix, $[D]$, is set equal to the identity matrix. Solving (25) in a least squares sense minimizes the following error function.

$$error(\theta) = \|[K_c]\{\theta\} - \{Q\}\|_2^2 + \|\Lambda[D]\{\theta\}\|_2^2 \tag{26}$$

This is the minimization of the residual plus a penalty term. The form of the damping matrix determines what penalty is used and the damping parameter, Λ, weights the penalty for each equation. These weights should be determined according to the error associated with the respective equation.

The regularization method uses Laplacian smoothing of the unknown temperatures and displacements only on the boundaries where the boundary conditions are unknown. This method could be considered a "second order" Tikhonov method. A penalty term can be constructed such that curvature of the solution on the unspecified boundary is minimized along with the residual.

$$\left\| \nabla^2 \theta_{ub} \right\|_2^2 \rightarrow min \tag{27}$$

For problems that involve unknown vector fields, such as displacements, Eqn. (27) must be modified to the following.

$$\left\| \nabla^2 \left(\hat{n} \cdot \{\delta_{ub}\} \right) \right\|_2^2 \rightarrow min \tag{28}$$

Here the normal component of the vector displacement field $\{\delta\}$ is minimized along the unknown surface.

Eqns. (27) and (28) can be discretized using the method of weighted residuals to determine the damping matrix, $[D]$.

$$\| [D]\theta_{ub} \|_2^2 = \| [K_c]\theta_{ub} \|_2^2 \tag{29}$$

In three-dimensional problems, [Kc] is computed by integrating over surface elements on the unknown boundaries. So the damping matrix can be thought of as an assembly of boundary elements that make up the boundary of the object where the boundary conditions are unknown. The stiffness matrix for each boundary element is formed by using a Galerkin weighted residual method that ensures the Laplacian of the solution is minimized over the unknown boundary surface. The main advantage of this method is its ability to smooth the solution vector without necessarily driving the components to zero and away from the true solution.

In general, the resulting FEM systems for inverse thermoelastic problems are sparse, unsymmetric, and often rectangular. These properties make the process of finding a solution to the system very challenging. One possible approach is to use iterative methods suitable for least squares problems. One such method is the LSQR method, which is an extension of the well known conjugate gradient (CG) method [31]. The LSQR method and other similar methods such as the conjugate gradient for least squares (CGLS) solve the normalized system, but without explicit computation of $[K]^T[K]$. These methods need only matrix-vector products at each iteration and therefore only require the storage of $[K]$ so they are attractive for large sized models. However, convergence rates of these methods depend strongly on the condition number of the normalized system that is the condition number of $[K]$ squared [32]. Therefore, solver performance degrades significantly as the size of the finite element model increases. Convergence can be slow when solving the systems resulting from the inverse finite element discretization since they are naturally ill-conditioned problems.

3.5 Numerical results

The accuracy and efficiency of the finite element inverse formulation was tested on several simple three-dimensional problems. The method was implemented in an object-oriented finite element code written in C++. Elements used in the calculations were of hexahedral shape with tri-linear interpolation functions. The linear systems were solved with a sparse LSQR method [31] with column scaling.

A simple test geometry was chosen to clearly demonstrate the approach. The test case involved a multiply-connected domain composed of an outer cylinder with length 5.0 m and diameter of 2.0 *m*. There are four cylindrical coaxial holes that pass completely through the cylinder, each with a diameter of 1.25 *m*. The

material domain was discretized using hexahedral computational mesh composed of 1440 elements and 1980 nodes. The inner and outer boundaries each had 440 nodes. For this multiply-connected geometry, there is no analytical solution, even if constant temperature boundary conditions are used on the boundaries.

This case considers thermal and elastic boundary conditions that vary in all coordinate directions thereby creating a truly three-dimensional example. The all interior boundary conditions change linearly along the z-axis. The exact values used are given in Table 1. On the outer cylinder the displacement was set to zero and a fixed temperature of 10 C was specified. Adiabatic and stress free conditions were specified at the ends of the cylinder. The following material properties were used: $E = 1.0 Pa$, $\nu = 0.0$, $\alpha = 2.0 \times 10^{-2} K^{-1}$, $k = 1.0 W\, m^{-1} K^{-1}$.

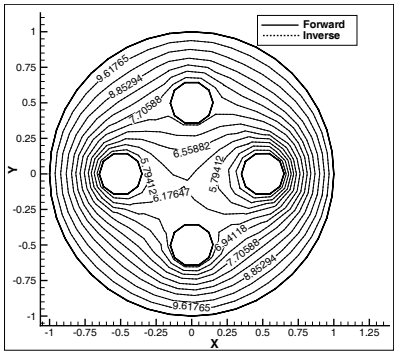

Fig. 4. Inversely computed isotherms on x - y plane at z = 0.5 m.

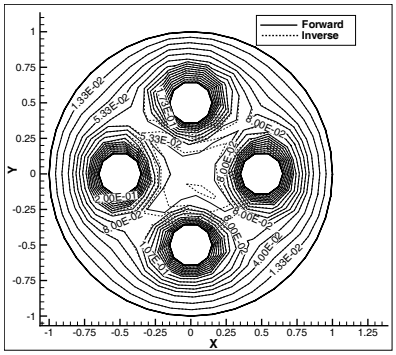

Fig. 5. Inversely computed displacement magnitudes on x - y plane at z = 0.5 m.

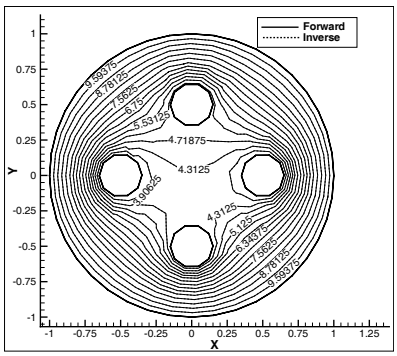

Fig. 6. Inversely computed isotherms on x - y plane at z = 2.5 m.

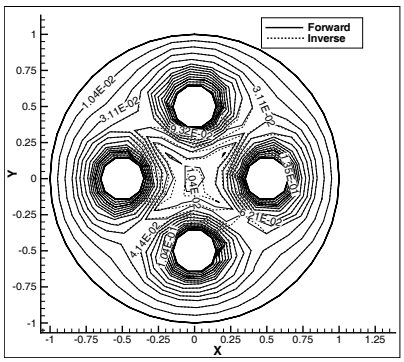

Fig. 7. Inversely computed displacement magnitudes on x - y plane at z = 2.5 m.

The inverse problem was generated by over-specifying the outer cylindrical boundary with the double-precision values of temperatures, fluxes, displacements, and surface tractions obtained from the forward analysis case. At the same time, no boundary conditions were specified on the inner cylindrical boundaries. No errors were used in the over-specified boundary data.

Table 1. Temperature and pressure boundary conditions for interior surfaces.

Hole	$T_{z-0}(°C)$	$T_{z-5}(°C)$	$P_{z-0}(Pa)$	$P_{z-5}(Pa)$
A	5.0	2.0	2.0	1.0
B	6.0	1.0	2.0	1.0
C	7.0	1.0	2.0	1.0
D	8.0	2.0	2.0	1.0

Regularization was used with $\Lambda = 8.5\times10^{-5}$. Our experience indicates that a good value for the damping parameter, Λ, is geometry and boundary condition dependent. Currently, the damping parameter is chosen based on experience by first choosing a small value and gradually increasing it until the numerical oscillations in the unknown boundary solution are removed.

The linear elasticity system was solved using the LSQR method with column scaling. The LSQR iterations were terminated after the Euclidean norm of the residual of the normal system was less than 1.0×10^{-6}. In this example 16805 LSQR iterations were required, which consumed about 10 minutes of computing time on a Pentium 4 workstation.

The average error between the inverse and direct solutions on the unknown boundaries was 0.02% for temperature and 5.6% for displacement. The direct and inverse temperature contours for two sections of the domain are shown in Figures 4 and 6. There is good agreement on all sections between the directly and inversely obtained isotherms. The direct and inverse constant displacement magnitude contours for three sections of the domain are shown in Figures 5 and 7. For all sections there is a noticeable difference in the direct and inverse contours in the regions far away from the outer boundary. However, the inverse solution does correctly capture the direct solution in a qualitative sense.

This thermoelastic problem was also solved using the other regularization methods over a wide range of damping parameters. In those cases the error in the inverse solution was much higher and did not match the direct solution even in a qualitative sense.

Improving the quality of the damping matrix for the displacement field could increase the accuracy of the displacement. The current damping matrix from Eqn. 28 only includes the normal component of the displacement. Smoothing the tangential components as well could make further improvements. In addition, the current scheme depends on accurate surface unit normal vectors, $\hat{n}$, which are difficult to compute accurately at the nodes of flat elements on curved surfaces. Further reductions in errors could possibly be made by implementing methods that compute the surface normals with a high degree of accuracy.

Reasonable results were obtained by LSQR with column scaling in less than 20,000 iterations for displacements and 3,000 iterations for temperature. Although many iterations are required with the LSQR method, it requires much less memory and is more robust than sparse direct solvers, such as QR factorization, for rectangular systems of algebraic equations.

This formulation can predict the temperatures and displacements on the unknown boundary with high accuracy using a proper regularization. It was shown that the FEM formulation could accurately predict unknown boundary conditions for multiply-connected domains when a good regularization scheme is used. Further research is needed to develop better regularization methods so that the present formulation can be made more robust with respect to measurement errors and more complex geometries. Further research is also needed to improve regularization for inverse problems in elasticity over complicated domains.

4 Inverse Design of Alloys for Specified Properties

Our research recently concentrated on the inverse method in predicting chemical composition of steel alloys. This formulation allows a structural design engineer who designed a machine part to ask a materials scientist to provide a precise chemical composition of an alloy that will sustain a specified stress level, σ_{spec}, at a specified temperature, T_{spec}, and last until rupture for a specified length of time, θ_{spec}. The inverse problem can be then formulated as a multi-objective optimization problem where a number of objectives are simultaneously minimized (Table 2). We have used IOSO multi-objective optimization algorithm [33, 34] which consists of two stages. The first stage is the creation of an approximation of the objective function(s). Each iteration in this stage represents a decomposition of the initial approximation function into a set of simple approximation functions (Fig. 1) so that the final response function is a multi-level graph [35, 36]. The second stage is the optimization of this approximation function. This approach allows for corrective updates of the structure and the parameters of the response surface approximation. The distinctive feature of this approach is an extremely low number of trial points to initialize the algorithm.

The result is not one, but a number of alloys (Pareto front points) each of which satisfying the specified properties while having different concentrations of each of the alloying elements. This is very practical because the user, when deciding to order an alloy, can use the alloy which is made of the most readily available and the most inexpensive elements on the market at that point in time.

In particular, the objective was to determine chemical composition(s) of high temperature steel alloys that will have specified (desired) physical properties. Design variables were concentrations (percentages) of each of the following 14 alloying elements C, S, P, Cr, Ni, Mn, Si, Mo, Co, Cb, W, Sn, Zn, Ti.

Table 2. Formulations for ten simultaneous objective functions in steel alloy design.

	Objectives (minimize simultaneously)			
Number of objectives	Operating Stress	Operating temperature	Time until rupture	Low cost alloy (minimize)
10	$(\sigma - \sigma_{spec})^2$	$(T - T_{spec})^2$	$(\theta - \theta_{spec})^2$	Ni, Cr, Nb, Co, Cb, W, Ti

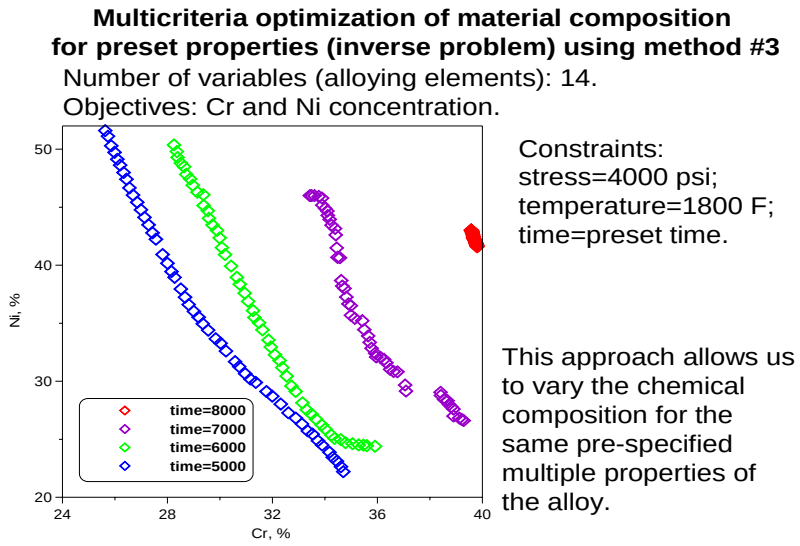

Fig. 8. Inversely designed Pareto optimal concentrations of Ni and Cr as a function of time –until-rupture constraint.

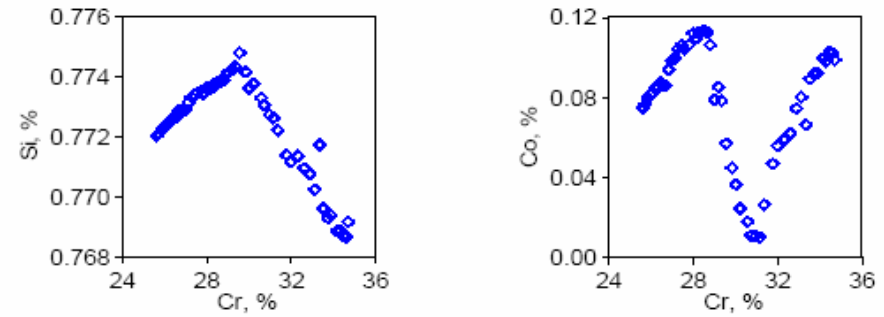

Fig. 9. Allowable variations of concentrations of S_i and C_o with respect to Cr when specifying stress (230 N mm^2), temperature (975 C) and time-to-rupture (5000 h).

Evaluations of the objectives were performed using classical experiments on candidate alloys. In other words, we used an existing experimental database. The results (Fig. 8) demonstrate that it is possible to create a large number of alloys having different compositions so that each of them will satisfy the specified multiple properties. This does not mean that concentrations vary smoothly for these alloys (Fig. 9). It should be pointed out that these are the visualizations of only two of the 14 chemical elements since the results of this multiple simultaneous least-square constrained minimization problem cannot be visualized for more that two alloying species at a time. Also, when T_{spec} and θ_{spec} progressively increase, the feasible ranges for varying the concentrations reduce rapidly [35].

Acknowledgements

The authors are grateful for the partial support provided by a grant from the US Army Research Office monitored by Dr. William M. Mullins and by a grant from the US Air Force Office of Scientific Research monitored by Dr. Todd E. Combs.

References

1. Beck JV, Arnold KJ (1977) Parameter Estimation in Engineering and Science, Wiley Interscience, New York, NY, USA
2. Kaipio J, Somersalo E (2004) Statistical and Computational Inverse Problems. Applied Mathematical Sciences, Springer-Verlag, **160**.
3. Alifanov OM (1977) Determination of Heat Loads from a Solution of the Nonlinear Inverse Problem. High Temperature **15**(3): 498-504
4. Alifanov OM (1994) Inverse Heat Transfer Problems, Springer-Verlag, New York
5. Alifanov OM (1974) Solution of an Inverse Problem of Heat-Conduction by Iterative Methods. J. Eng. Physics **26**(4): 471-476
6. Artyukhin EA, Nenarokomov AV (1988) Coefficient Inverse Heat Conduction Problem. J. Eng. Physics **53**: 1085-1090
7. Alifanov OM, Mikhailov VV (1983) Determining Thermal Loads from the Data of Temperature Measurements in a Solid. High Temperature **21**(5): 724-730
8. Alifanov OM, Rumyantsev SV (1979) On the Stability of Iterative Methods for the Solution of Linear Ill-Posed Problems. Soviet Math. Dokl., **20**(5): 1133-1136
9. Alifanov OM, Rumyantsev SV (1980) Regularizing Gradient Algorithms for Inverse Thermal-Conduction Problems. J. Eng. Physics **39**(2): 858-861
10. Alifanov OM, Tryanin AP (1985) Determination of the Coefficient of Internal Heat Exchange and the Effective Thermal Conductivity of a Porous Solid on the Basis of a Nonstationary Experiment. J. Eng. Physics **48**(3): 356-365
11. Alifanov OM, Artyukhin E, Rumyantsev A (1995), Extreme Methods for Solving Ill-Posed Problems with Applications to Inverse Heat Transfer Problems, Begell House, New York, NY, USA
12. Artyukhin EA (1981) Reconstruction of the Thermal Conductivity Coefficient from the Solution of the Nonlinear Inverse Problem. J. Eng. Physics **41**(4): 1054-1058
13. Artyukhin EA (1993) Iterative Algorithms for Estimating Temperature-Dependent Thermophysical Characteristics. In Proc. of 1st International Conference on Inverse Problems in Engineering – Proceedings, Palm Coast, FL, USA: 101-108
14. Artyukhin EA, Rumyantsev SV (1981) Descent Steps in Gradient Methods of Solution of Inverse Heat Conduction Problems. J. Eng. Physics **39**: 865-868
15. Alifanov OM (2002) Mathematical and Experimental Simulation in Designing and Testing Heat-Loaded Enginering Objects, In Proc. of the Inverse Problems in Engineering: Theory and Practice – Vol. I, (Orlande, H. R. B. Editor), e-papers Publishing House, Rio de Janeiro, Brazil: 13-21
16. Özisik MN, Orlande HRB (2000) Inverse Heat Transfer: Fundamentals and Applications, Taylor & Francis, New York, NY, USA
17. Silva PMP, Orlande HRB, Colaço MJ, Shiakolas PS, Dulikravich GS (2005) Estimation of Spatially and Time Dependent Source Term in a Two-Region Problem**.** In Proceedings of the 5th International Conference on Inverse Problems in Engineering: Theory and Practic (Lesnic, D. ed.) July 11-15, 2005, Cambridge, United Kingdom

18. Dennis BH, Dulikravich GS (1999) Simultaneous Determination of Temperatures, Heat Fluxes, Deformations, and Tractions on Inaccessible Boundaries. ASME Journal of Heat Transfer **121**: 537–545
19. Dennis BH, Dulikravich GS (2001) A 3-D Finite Element Formulation for the Determination of Unknown Boundary Conditions in Heat Conduction. In Proc. of Internat. Symp. on Inverse Problems in Eng. Mechanics, Tanaka M, Ed., Nagano City, Japan
20. Dennis BH, Dulikravich GS, Han ZX (2004) Determination of Temperatures and Heat Fluxes on Surfaces and Interfaces of Multi-domain Three-Dimensional Electronic Components, ASME Journal of Electronic Packaging **126** (4): 457-464
21. Dennis BH, Dulikravich GS, Yoshimura S (2004) A Finite Element Formulation for the Determination of Unknown Boundary Conditions for 3-D Steady Thermoelastic Problems. ASME Journal of Heat Transfer **126**: 110–118
22. Larsen ME (1985) An Inverse Problem: Heat Flux and Temperature Prediction for a High Heat Flux Experiment. Tech. report SAND-85-2671, Sandia National Laboratories, Albuquerque, NM, USA
23. Hensel EH, Hills R (1989) Steady-State Two-Dimensional Inverse Heat Conduction. Numerical Heat Transfer **15**: 227–240
24. Martin TJ, Dulikravich GS (1996) Inverse Determination of Boundary Conditions in Steady Heat Conduction with Heat Generation. ASME J. of Heat Transfer **3**: 546–554
25. Olson LG, Throne RD (2000) The Steady Inverse Heat Conduction Problem: A Comparison for Methods of Inverse Parameter Selection. In Proc. of the 34th ASME National Heat Transfer Conference-NHTC'00, NHTC2000-12022, Pittsburg, PA, USA
26. Martin TJ, Halderman J, Dulikravich GS (1995) An Inverse Method for Finding Unknown Surface Tractions and Deformations in Elastostatics. Computers and Structures **56**: 825–836.
27. Martin TJ, Dulikravich GS (1995) Finding Temperatures and Heat Fluxes on Inaccessible Surfaces in 3-D Coated Rocket Nozzle. In 1995 JANNAF Non-Destructive Evaluation Propulsion Subcommittee Meeting, Tampa, FL, USA: 119–129
28. Huebner KH, Thorton EA, Byrom TG (1995) The Finite Element Method for Engineers. John Wiley and Sons, third edition, New York, NY, USA
29. Hughes TJR (2000) The Finite Element Method: Linear Static and Dynamic Finite Element Analysis. Dover Publications, Inc., New York, NY, USA
30. Neumaier A (1998) Solving Ill-Conditioned and Singular Linear Systems: A Tutorial on Regularization. SIAM Review **40**: 636–666
31. Paige CC, Saunders MA (1982) LSQR: An Algorithm for Sparse Linear Equations and Sparse Least Squares. ACM Transactions on Mathematical Software **8**: 43–71
32. Saad Y (1996) Iterative Methods for Sparse Linear Systems. PWS Publishing Co., Boston, MA, USA
33. Egorov IN, Kretinin GV (1992) Multicriterion stochastic optimization of axial compressor. In Proc. of ASME COGEN-TURBO-VI, Houston, TX, USA
34. Egorov IN, Kretinin GV, Leshchenko IA, Kostiuk SS (1999) The methodology of stochastic optimization of parameters and control laws for the aircraft gas-turbine engines flow passage components. ASME paper 99-GT-227, June 3-7, Indianapolis, IN, USA
35. Egorov IN, Dulikravich GS (2004) Inverse design of alloys for specified stress, temperature and time-to-rupture by using stochastic optimization. In Proc. of the International Symposium on Inverse Problems, Design and Optimization – IPDO; Colaco MJ, Dulikravich GS, Orlande HRB, eds.; March 17-19, Rio de Janeiro, Brazil
36. Yegorov-Egorov IN, Dulikravich GS (2005) Chemical composition design of superalloys for maximum stress, temperature and time-to-rupture using self-adapting response surface optimization. Materials and Manufacturing Processes **20** (3): 569-590